Measurements of the mechanical behaviour of micromachined silicon and silicon-nitride membranes for microphones, pressure sensors and gas flow meters

R. Schellin, G. Hess, W Kuhnel, C. Thielemann, D. Trost and J. Wacker
Institut fur Ubertragungstechnik und Elektroakustik, Technische Hochschule Darmstadt, 64283 Darmstadt (Germany)

R. Steinmann
Institut fur Stahlbau und Werkstoffmechanik, Technische Hochschule Darmstadt, 64283 Darmstadt (Germany)

Abstract

This paper mainly presents the experimental determination of the small deflection behaviour of boron-implanted silicon-nitride and highly boron-doped silicon diaphragms for micromachined silicon subminiature microphones The additional implantation of boron into silicon-nitride diaphragms reduces the intrinsic stress in the deposited amorphous films The minimum detectable deflection, using a Mach–Zehnder interferometer, is about 0 02 nm for dynamic measurements (A-weighted filtering) The largest measurable deflection (where nonlinearities of the interferometer are negligible) is strongly influenced by the wavelength of the laser and is about 10 nm Thus, applying this method to pressure sensors and gas flow meters, the pressure range is restricted In order to achieve a high sensitivity of the measuring apparatus and a low detectable deflection amplitude a feedback configuration stabilizes the interferometer in the most sensitive operation points

1. Introduction

In order to reduce the geometric dimensions of physical, biological, electrochemical and medical sensors, microelectronic and micromechanical fabrication technologies are required In the last 15 years a great variety of sensors using the fabrication procedures mentioned above has been developed, especially pressure sensitive silicon sensors as microphones, pressure sensors and gas flow meters (see, e g , refs 1–3) Common to all these sensors is the use of a very thin and small silicon or silicon-nitride membrane In order to determine the mechanical behaviour of these membranes, measurements of the deflection behaviour in the case of applied pressure or airborne sound must be performed

Several experimental investigations were previously developed in order to determine the technological and elastic parameters and, therefore, the mechanical behaviour of silicon and silicon-nitride membranes, e g , determination of the bending of the wafer [4], determination of the resonance frequency of silicon beams and measurements of the deflection amplitude of silicon beams and silicon diaphragms [5] In order to achieve a nearly full understanding of the mechanical behaviour of silicon and silicon-nitride diaphragms, the exact determination of the deflection behaviour is absolutely necessary Especially the investigation of the combined action of applied pressure/airborne sound and in-plane stress due to thermal mismatch and intrinsic stress due to dislocations, etc , is of great interest (see, e g , refs 6 and 7)

The determination of the elastic constants and/or the in-plane stress requires special conditions during measurements (e g , high pressure [5, 8]) in combination with curve-fitting procedures Furthermore, the combined action of plate-like or membrane-like deflection behaviour is difficult to separate With respect to the deflection behaviour, special optical displacement measurement techniques (e.g , measurements of the deflection with a modified Michelson interferometer [9]) are quite promising A different possibility is presented here A stabilized Mach–Zehnder interferometer is used to meet the following requirements· accuracy of measurement, bandwidth, sensitivity, low noise level

Since the sensitivity of a Mach–Zehnder interferometer is very high, very low deflection amplitudes in the low frequency range (up to 100 kHz) are detectable The low noise level and the high accuracy are obtained by the use of the stabilizing feedback configuration 'D c -deflection' measurements are always influenced by thermal drift effects or high noise level due to vibration disturbances Therefore, dynamical measure-

SSDI 0924-4247(93)00476-K

ments are favoured due to the possibility of compensating for the undesired effects mentioned above

In order to compare the measurement results with theoretical predictions in the second section of this paper some basic theoretical considerations about the deflection behaviour of diaphragms for silicon microphones are given Assuming static or quasi-static pressure changes, these considerations are also valid for pressure sensors and gas flow meters Especially the deflection amplitudes in the case of pure plate and pure membrane behaviour are presented The main part of the paper deals with the description of the measuring principle to determine the deflection behaviour of the thin diaphragms In Section 4 the fabrication of silicon-nitride and silicon membranes by wet-etching in KOH solution is described A special boron implantation process is used in order to reduce the in-plane stress of the silicon-nitride layers Experimental results concerning the measurements of the deflection amplitudes are presented in Section 5 Especially the influence of the additional boron implantation of the silicon-nitride membranes is shown

2. Deflection behaviour of the diaphragms

The deflection behaviour of a silicon diaphragm below its resonance frequency can be determined by applying standard plate theory This leads to the following differential equation for the displacement $w(x, y)$ of an orthotrophic plate (here $E_x = E_y = E$) including in-plane stress [10]

$$D\frac{\partial^4 w}{\partial x^4} + 2H\frac{\partial^4 w}{\partial x^2 \partial y^2} + D\frac{\partial^4 w}{\partial y^4} + Th\left(\frac{\partial^2 w}{\partial x^2} + \frac{\partial^2 w}{\partial y^2}\right) = p \qquad (1)$$

with $D = Eh^3/12(1-\nu^2)$, $D_1 = D\nu$, $D_{xy} = Gh^3/12$ and $H = D_1 + 2D_{xy}$, the thickness h, Poisson's ratio ν, the elasticity moduli E and G, and T the homogeneous in-plane stress For a square silicon membrane of area a^2 this equation can only be solved numerically by satisfying the following conditions for a rigidly clamped plate

$$w(x=0, a\,y) = 0, \qquad w(x.y=0, a) = 0$$
$$\left.\frac{\partial w}{\partial x}\right|_{x=0\ a\ y} = 0, \qquad \left.\frac{\partial w}{\partial y}\right|_{x\ y=0,\ a} = 0 \qquad (2)$$

Several methods are applicable, such as FEM simulation, Rayleigh–Ritz method, finite difference method, etc (a comprehensive overview of the methods mentioned above is given in ref 10) Neglecting in-plane stress, good consistency between experimental and theoretical results is achievable by applying a 'direct-solution method' [11] Including in-plane stress, the results obtained by the latter method are more or less accurate, depending on the amount of in-plane stress

Much simpler, but still with sufficient accuracy, the deflection behaviour of a square diaphragm of area A can be approximated by the deflection of a circular diaphragm with the same area [12] For an isotropic, circular, clamped diaphragm with plate behaviour and additional in-plane stress, the static deflection amplitude of pure plates (low tension) and pure membranes (high tension) as a function of in-plane stress can be expressed by [13]

(a) *Pure plate behaviour*

$$w_{\text{plate}}(r) = \frac{pa^4}{64D}\left[1 - \left(\frac{r}{a}\right)^2\right]^2 \qquad (3)$$

(b) *Pure membrane behaviour*

$$w_{\text{memb}}(r) = \frac{p}{Th}\left[\frac{a^2 - r^2}{4}\right] \qquad (4)$$

where $D = Eh^3/12(1-\nu^2)$ is the flexural strength of the diaphragm, a the radius and r the distance from the centre of the membrane

3. Mach–Zehnder interferometer

3 1 Basic configuration

The basic configuration of the present interferometer is shown in Fig 1 The interferometer is based on a standard Michelson interferometer extended by an additional beam splitter, an additional photodetector and a feedback configuration in order to stabilize the interferometer in the most sensitive operation point Just prior to passing the primary beam splitter, the emitted laser light (He/Ne laser, 633 nm wavelength) is diverged in order to allow a better focusing of laser light onto the silicon sample 50% of the laser light, crossing the first beam splitter, is divided again into two separate laser beams by the second beam splitter One of the

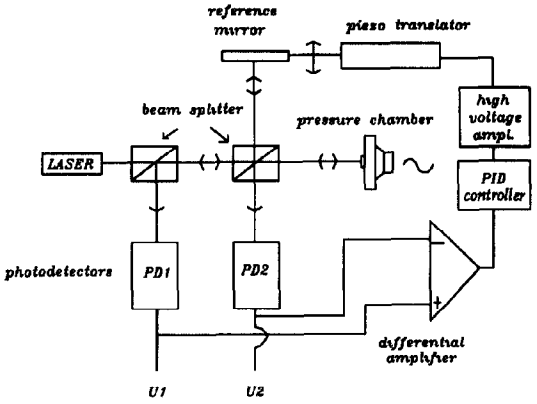

Fig 1 Mach–Zehnder interferometer with active phase-tracking system (lenses and microscope objectives are omitted)

beams (sample beam) is focused onto the silicon diaphragm, the other one serves as a reference beam and is reflected by the piezo-driven mirror From each laser beam, one part is deflected in the direction of photodiode amplifier 1 (primary laser beam), the other part passes the secondary beam splitter and is deflected in the direction of photodiode amplifier 2 (secondary laser beam) They superimpose and an interference pattern is visible on the front side of the photodiode amplifiers Since the secondary beam is phase-shifted by an amount π, the output signals of the two current–voltage converters are also phase-shifted by an amount π

3 2 Contrast transfer functions of the interferometer and determination of the deflection amplitude of the diaphragms

The contrast transfer functions of the interferometer are shown in Fig 2 Since the deflection of the silicon diaphragm of a silicon subminiature microphone in the case of applied airborne sound is much smaller than the wavelength of the laser, the dynamic phase shift of the sample beam leads to a 'small-signal operation' of the interferometer

The total intensity at one photodector is given by

$$I_{\text{total 1}} = I_0(1+\cos\,\phi) \tag{5}$$

where ϕ is the static phase difference between the beam deflecting on the sample surface and the reference beam For the other photodetector the following equation for the total intensity is valid

$$I_{\text{total 1}} = I_0[1+\cos(\phi+\pi)] \tag{6}$$

The derivative of the transfer function with respect to the phase shift of the first detector leads to

$$\frac{\partial I_{\text{total 1}}}{\partial \phi} = -I_0 \sin\,\phi \tag{7}$$

Its maximum value I_0 is obtained for $\phi=(2n+1)\pi/2$, $n=0, 1, 2,$ or (changing from differentials to finite differences, which is allowed in the quadrature point)

$$\left|\frac{\Delta I_{\text{total 1}}}{I_0}\right| = \Delta\phi \tag{8}$$

where $\Delta\phi$ is the dynamic phase shift The deflection amplitude w of the diaphragm may be obtained by

$$2w = \frac{\lambda/2}{2\pi}\,\Delta\phi \tag{9}$$

since a deflection amplitude of w results in a difference of $2w$ in the optical path length

Finally, the deflection (in nm) is

$$w = 25\,15\Delta\phi = 25\,15\left|\frac{\Delta I_{\text{total 1}}}{I_0}\right| \tag{10}$$

where $\lambda = 633$ nm, $\Delta I_{\text{total 1}}$ is the peak-to-peak value of the a c component of the output signal and $2I_0$ the difference between the maximum and the minimum d c output voltage of one photodetector

3 3 Active phase-tracking

In order to obtain a stabilized interferometer an active phase-tracking system is used [14] It is based on the fact that at the most sensitive operating points (see Fig 2 points A and B) the d c output values of the photodiode amplifiers are the same Subtracting the output signals of both photodiode amplifiers leads to a vanishing d c value and doubles the a c value due to the phase shift of π Therefore, the vanishing d c value can be used to stabilize the interferometer by the feedback configuration seen in Fig. 1

The output signal of the differential amplifier passes a proportional plus floating plus derivative control (PID control) and is amplified by a high-voltage amplifier Applying it to a high voltage piezo-translator, the reference mirror is moved in such a way that the output signal of the differential amplifier is regulated to zero This feedback configuration increases significantly the minimum detectable deflection amplitude of the interferometer, since thermal drift effects and low frequency disturbances are reduced Furthermore, a much better linearity is achieved

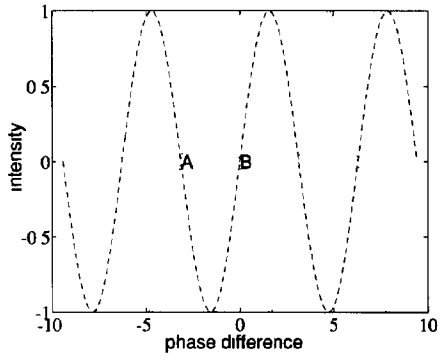

Fig 2 Contrast transfer functions of the Mach–Zehnder interferometer photodetector 1, – – –, photodetector 2

4. Fabrication of silicon-nitride and silicon diaphragms

4 1 Fabrication of the silicon diaphragms

The silicon diaphragms consist of a highly boron-doped silicon layer, formed by a predeposition process, masked by a thick silicon-dioxide layer After etching away this masking silicon-oxide film, a thin stress-reducing layer of silicon dioxide is fabricated by a dry thermal oxidation On top of this layer (rear and front

side of the wafer) a silicon-nitride layer of approximately 150 nm thickness is deposited This composite layer system is used in order to prevent a cracking of the silicon-nitride film The top side is covered with a hardened photoresist and on the rear side photolithography is performed using a two-sided mask aligner After patterning of the silicon-nitride/silicon-dioxide layer system inside the open photoresist window on the rear side of the wafer, the membrane is fabricated This is done by a wet-etch in potassium hydroxide Now the silicon-nitride/silicon-dioxide layer system on the top side of the wafer is removed and the diaphragms are metallized with a 100 nm thick aluminium layer The resulting silicon diaphragm has a thickness of about 1 μm and an area of about 1 mm^2

4 2 Fabrication of the silicon-nitride diaphragms

The silicon-nitride diaphragms consist of an APCVD or LPCVD silicon nitride First a stress-reducing layer of silicon dioxide (which is under compressive stress) is fabricated by a dry thermal oxidation On top of this layer (rear and front side of the wafer) a silicon-nitride film of approximately 150 nm thickness is deposited (APCVD $T \approx 2\,3 \times 10^9$ N/m^2, LPCVD $T \approx 3 \times 10^8$ N/m^2) The top side is covered with a hardened photoresist and on the rear side photolithography is performed using a two-sided mask aligner After patterning of the silicon-nitride/silicon-dioxide layer system inside the open photoresist window on the rear side of the wafer, the photoresist is etched away and a boron implantation is performed on the top side of the wafers This special process step is introduced in the fabrication procedure in order to reduce further the total in-plane stress of the diaphragms [15] Subsequently the diaphragms are fabricated by a wet-etch procedure in potassium hydroxide and finally they are metallized by a 100 nm aluminium layer

5. Experimental results and discussion

5 1 Capabilities of the measurement apparatus

The measurement of the deflection amplitude of a thin diaphragm requires a good sensitivity, low noise level and good linearity of the interferometer

Its sensitivity (output voltage of one photodetector) is about 7 mV/nm This high value allows a further amplification without any problems concerning noise level

In addition to the sensitivity another important parameter influencing the performance of a measuring apparatus is the minimum detectable signal (MDS) level (in dB) The MDS level for a given bandwidth may be written as

$$\text{MDS level} = L_w - 20 \log \frac{S}{N}$$

$$= L_w - 20 \log \frac{U_s(w)}{U_r} \qquad (11)$$

where $U_s(w)$ is the signal voltage, L_w the deflection level with respect to an amplitude of 1 nm and U_r is the noise voltage For a deflection amplitude of 1 nm (measuring frequency 1 kHz) an A-weighted signal-to-noise ratio (S/N) of about 50 was measured From these values a minimum detectable signal level of about -33 dB (ref to 1 nm, A-weighted) and therefore a minimum detectable deflection amplitude of about 0 02 nm were achieved This may be increased by the use of bandpass filters and/or lock-in-detection techniques Using eqn (10), an A-weighted phase shift $\Delta\phi$ of 8×10^{-4} rad was detectable

The linearity of the interferometer was measured by exciting the piezo-driven reference mirror sinusoidally to vibrations with different amplitudes and observing the unfiltered output signal of the photodetectors with a spectrum analyser An excellent linearity could be achieved for deflection amplitudes less than 5 nm (nonlinear distortion factors 0 25 and 1 8% for a deflection amplitude of 0 5 and 5 nm, respectively)

5 2 Deflection amplitudes of the diaphragms

The deflection amplitude of a silicon-nitride membrane with a tensile stress of about $5\,8 \times 10^7$ N/m^2 (the stress values have been determined by using a mechanical profilometer [16]) as a function of frequency of the airborne sound pressure was measured A flat frequency response in the whole audio frequency range was obtained

Furthermore, the deflection amplitude as a function of sound pressure (see Fig 3) at a frequency of 1 kHz is shown, which is highly linear for silicon-nitride mem-

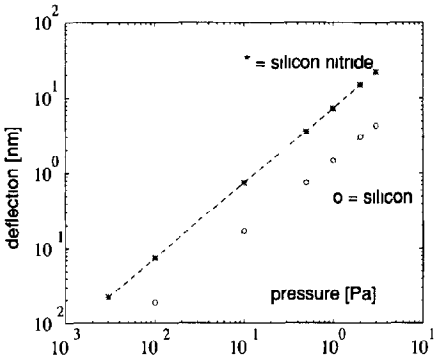

Fig 3 Deflection amplitude of silicon-nitride and silicon diaphragms as a function of airborne sound pressure (measurement frequency 1 kHz)

branes and silicon diaphragms Due to a lower in-plane stress of the silicon-nitride diaphragms and a smaller thickness they show a much higher deflection amplitude

In Fig 4 the centre deflection amplitude as a function of in-plate stress of a silicon-nitride membrane is shown It is compared with simulation results based on the equations of Section 2 and using a value of the total centre deflection ($r=0$) amplitude of

$$\frac{1}{w_{\text{total}}} = \frac{1}{w_{\text{plate}}} + \frac{1}{w_{\text{memb}}} \tag{12}$$

or using eqns (3) and (4)

$$w_{\text{total}} = \frac{pa^4}{64D} \frac{1}{1+\frac{a^2}{16}\frac{Th}{D}} \tag{13}$$

Good agreement between the measured and simulated results was obtained The differences may be explained by the measurements of the in-plane stress and of the thickness of the diaphragm (210 nm, considering the aluminium layer on top of the silicon-nitride membrane) and by the assumption of a circular diaphragm of the same area (radius a of 0 564 mm leads to 1 mm^2) compared to the real square shape of the diaphragms The influence of the assumed values for Young's modulus ($2\,09\times10^{11}$ N/m^2) and Poisson's ratio (0 28) [17] must not be considered, since the measured membranes are in the high tensile stress region, where plate effects may be neglected

The different values of in-plane stress mentioned above could be achieved by performing different boron implantations into or through the silicon-nitride membranes In Fig 5 three different implantation energies with different implantation doses are shown The upper curves correspond to an APCVD-deposited silicon-nitride film, whereas the two other curves represent measurements of LPCVD-deposited silicon-nitride films Both layers were fabricated using silicon dioxide as a stress-reducing support Obviously, the reduction

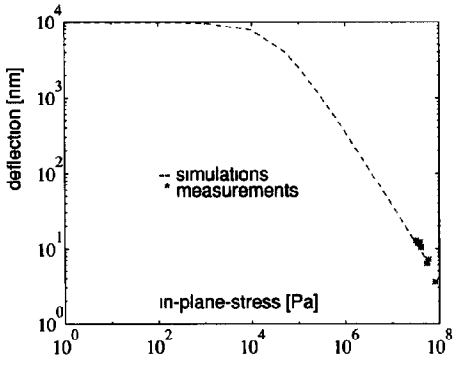

Fig 4 Deflection amplitude of a silicon-nitride diaphragm as a function of in-plane stress T at a constant pressure p

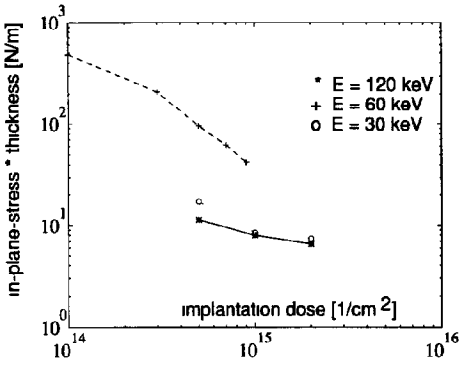

Fig 5 In-plane stress of silicon-nitride diaphragms (LPCVD lower curves, APCVD upper curve) as a function of boron implantation dose, parameter E is the implantation energy

in in-plane stress is larger for higher implantation doses The dependence on implantation energy is not so important (comparing the two lower curves) Thus, to achieve a low in-plane stress in order to obtain more flexible membranes, it is very important to choose proper implantation conditions

6. Conclusions

A method to measure very small deflections (down to 0 02 nm) of silicon and silicon-nitride diaphragms was presented The measurements of the diaphragms were performed in the audio frequency range in order to achieve a good signal-to-noise ratio during the measurements This is much easier, since thermal drift effects and low frequency disturbances are reducible simply by filtering

Furthermore, the influence of boron implantation into silicon-nitride diaphragms on the in-plane stress of such layers has been shown Low stress values could be obtained by high dose implantation Nevertheless the total in-plane stress (intrinsic stress, stress due to thermal mismatch of the layer system mentioned above with respect to the silicon substrate and the additional compressive stress which is incorporated by the boron implantation) is still tensile For most sensor applications this is a desirable result, in order to avoid buckling of the micromachined structures Especially for silicon microphones a net amount of tensile stress is necessary to achieve resonance frequencies of about 20 kHz

The present interferometer set-up provides the possibility of the determination of in-plane stress with a high accuracy over a wide dynamic range (0 02 up to 10 nm) up to frequencies of about 10 kHz

The goal of future work is the refinement of the present interferometer set-up by using more enhanced filter techniques (e g , lock-in amplification) in order

to achieve a lower minimum detectable deflection amplitude – especially for measurements in the edge region of the membrane and for measurements of the shape of the diaphragm deflection – and therefore a higher signal-to-noise ratio This allows much better predictions of the mechanical properties of micromachined silicon sensors with thin diaphragms, especially with respect to the elasticity coefficients (plate region), the in-plane stress (membrane region), etc

Acknowledgements

This work was supported by the 'Deutsche Forschungsgemeinschaft' The authors would especially like to thank Professor G M Sessler for helpful discussions and the staff of the Institute for Semiconductor Technology of the Technical University of Darmstadt and the staff of the Fraunhofer Institute in Berlin for the fabrication of the diaphragms

References

1 R Schellin and G Hess, A silicon subminiature microphone based on piezoresistive polysilicon strain gauges, *Sensors and Actuators A, 32* (1992) 555–559
2 V A Gridchin, V M Lubimskyi and M P Sarina, Polysilicon strain-gauge transducers, *Sensors and Actuators A, 30* (1992) 219–223
3 S T Cho, C E Lowman and K D Wise, An ultrasensitive silicon pressure-based microflow sensor, *IEEE Trans Electron Devices, ED-39* (1992) 825–835
4 E I Bromley, J N Randall, D C Flanders and R W Mountain, A technique for the determination of stress in thin films, *J Vac Sci. Technol. B, 1* (1983) 1364–1366
5 O Tabata, K. Kawahate, S Sugiyama and I Igarashi, Mechanical property measurements of thin films using load deflection of composite rectangular membranes, *Sensors and Actuators, 20* (1989) 135–141
6 J A Voorthuyzen and P Bergveld, The influence of tensile forces on the deflection of circular diaphragms in pressure sensors, *Sensors and Actuators, 6* (1984) 201–213
7 P Scheeper, A silicon condenser microphone materials and technology, *Ph D Thesis,* University of Twente, 1993
8 B Puers and S Vergote, A subminiature capacitive movement detector using a composite membrane suspension, *Sensors and Actuators A, 31* (1992) 90–96
9 R Keller, R Salathe, T Tschudi and C Voumard, Michelson interferometer for detection of fast displacements of less than a quarter-wave over small areas, *Appl. Opt, 14* (1975) 1616–1620
10 R Szilard, *Theory and Analysis of PLATES,* Prentice-Hall, Engelwood Cliffs, NJ, 1974
11 S Timoshenko and S Woinowsky-Krieger, *Theory of Plates and Shells,* McGraw-Hill, New York, 2nd edn, 1959
12 J Maisano, More advanced models for silicon condenser microphones, Paper presented at *92nd Convention of the Audio Engineering Society, Vienna, Austria, Mar 24–27, 1992*
13 W P Mason, *Electromechanical Transducers and Wave Filters,* Van Nostrand Reinhold, New York, 2nd edn, 1948
14 D A Jackson, A Dandridge and S K. Sheem, Measurement of small phase shifts using a single-mode optical-fiber interferometer, *Opt Lett, 5* (1980) 139–141
15 E P EerNisse, Stress in ion-implanted CVD silicon-nitride films, *J Appl Phys, 48* (1977) 3337–3341
16 K.E Growe and R L Smith, A new technique for determination of tensile stress in thin films, *J Electrochem Soc, 136* (1989) 1566
17 W Kühnel, Kapazitive Siliziummikrofone, *Ph D Thesis,* Technical University Darmstadt, 1992